

## Strong coupling operation of a free-electron-laser amplifier with an axial magnetic field

J. L. Rullier, A. Devin, J. Gardelle, J. Labrouche, and P. Le Taillandier  
*Commissariat à l'Energie Atomique, Boîte Postale 2, 33114 Le Barp, France*

J. T. Donohue

*Centre d'Etudes Nucléaires de Bordeaux-Gradignan, Boîte Postale 120, 33175 Gradignan, France*

(Received 16 October 1995)

We present the results of a free-electron-laser (FEL) experiment at 35 GHz, using a strongly relativistic electron beam ( $T=1.75$  MeV). The electron pulse length is 30 ns full width at half maximum with a peak current of 400 A. The FEL is designed to operate in the high-gain Compton regime, with a negative coupling parameter ( $\Phi < 0$ ) leading to a strong growth rate. More than 50 MW of rf power in the TE<sub>11</sub> mode (43 dB gain) has been obtained with good reproducibility. The experimental results are in good agreement with predictions made using the three-dimensional stationary simulation code SOLITUDE.

PACS number(s): 41.60.Cr, 52.75.Ms, 41.85.Ja, 41.85.Lc

### I. INTRODUCTION

Free-electron lasers (FELs) have been extensively investigated over the last 20 years because of their remarkable properties, which include high efficiencies and output powers, their potential as sources of coherent short wavelength radiation, and their inherent frequency tunability. A presentation of much of the FEL research carried out prior to 1992 may be found in the monograph of Freund and Antonsen [1]. Several experiments have been carried out using a helical wiggler [2–11], as in the present experiment. Some FELs operate at moderately high beam current and use a magnetic guide field  $B_0$  to steer the electron beam in the axial direction. For that experimental setup, the one-dimensional analysis of the FEL operation predicts that a resonance occurs when the cyclotron wavelength  $\lambda_0 = 2\pi\beta_{\parallel}c/\Omega_0$  in the axial magnetic field approaches the wiggler periodicity  $\lambda_w$  [12,13] [here  $\Omega_0 = |e|B_0/m\gamma$  is the relativistic cyclotron frequency,  $e$  and  $m$  denote the charge and mass of the electron,  $\gamma = (1 - \beta_{\parallel}^2 - \beta_{\perp}^2)^{-1/2}$  is the relativistic energy factor and  $\beta_{\perp}$  and  $\beta_{\parallel}$  are the dimensionless transverse and axial velocities corresponding to the helical trajectories which the electrons are supposed to follow]. In fact, the more accurate analysis of Freund and Ganguly [14], which takes into account the radial variation of the wiggler magnetic field, shows that the resonance cannot, in fact, be obtained. Thus the FEL can run either in the group I regime, with  $\lambda_0 > \lambda_w$ , or in the group II regime, with  $\lambda_0 < \lambda_w$ . As the resonant condition is approached, from either side, the helical orbits become unstable and the electrons strike the walls.

These experiments can be made to operate in the high gain regime. Early theoretical work by Freund *et al.* [13] (using the one-dimensional approximation), and by Freund and Ganguly [14] in their more precise three-dimensional (3D) analysis, has shown the importance of the coupling parameter they call  $\Phi$ . The coefficient of the growth of the electromagnetic wave is predicted to be

proportional to  $\Phi$ . Since the one-dimensional and the three-dimensional forms of this quantity are quite different in the group II regime, we shall use only the latter, as given in Ref. [14]. It has been suggested that it would be of interest to operate with a negative value of  $\Phi$  even though the space charge wave is more unstable [13]. In this paper we report the results of an experiment using a strongly relativistic electron beam, with parameters which may be adjusted so as to obtain large negative values of  $\Phi$ . It was designed to run amplifying a magnetron signal at the frequency of 35.1 GHz, although some observations in the superradiant mode (with the magnetron turned off) were also carried out.

Experiments similar in design to the present one, and which amplified a signal at frequencies near 35 GHz, were carried out several years ago, notably at the Naval Research Laboratory [15,16]. A detailed review of this work is given in Ref. [6]. One may then ask what additional lessons, if any, can be learned from the present experiment. While ours is indeed similar to those earlier experiments, a major difference concerns the physical size of the apparatus. The early experiments used generators of somewhat lower voltage than ours, and they functioned with waveguides whose diameters were approximately 10 mm. Our experiment, for technical reasons, required a somewhat larger scale. In consequence it was capable, at least in theory, of exploring domains of the operating parameter space which the previous experiments had not investigated, in particular, large negative values of the coupling parameter  $\Phi$ . The exploration of this regime was the principal aim of this experiment. To some extent, the conclusions to be drawn from it are negative, since despite the higher values of  $\Phi$  that were obtained, no corresponding increase in output power was observed, compared to the earlier experiments. We shall present in Sec. III a brief comparison between our results and those of Ref. [15].

Experimental results for various values of the wiggler field and the axial guide field have been obtained. In the amplifier regime a maximum output power radiation of

50 MW has been reached which corresponds to an efficiency of 7%. A study of the saturation as a function of the wiggler length has been carried out. The experimental results have been compared with the numerical computations provided by the particle simulation code SOLITUDE [17,18], and good agreement has been found.

## II. EXPERIMENT

A schematic of the FEL amplifier experiment is shown in Fig. 1. The main components of the device are the pulsed-line generator Euphrosyne, the graphite diode, the axial guiding solenoid, and the bifilar wiggler. The accelerating voltage for the experiment is supplied by a Marx capacitor bank with a Blumlein transmission line delivering a 1.75 MV, 50 ns pulse. The strongly relativistic electron beam is emitted from a hemispherical graphite cathode by field emission (microexplosive emission process). The graphite anode, with its 3.5 mm radius aperture, is 60 mm long. It allows only a small fraction of the current to propagate and acts as an emittance selector. Typical measurements of the voltage and the current as a function of time are illustrated in Fig. 2. Making use of the calculation of Ref. [19] we can establish an upper limit on the geometrical emittance  $\epsilon$  of  $550\pi$  mm mrad.

The bifilar helical wiggler consists of 28 periods of length  $\lambda_w = 8$  cm and provides a magnetic field whose magnitude  $B_w$  on axis is adjustable up to 3 kG. With the use of the metallic straps between helically wound wires, the wiggler field is slowly uptapered over the first eight periods. This provides an adiabatic input into the interaction region for the electron beam. The diode and the wiggler, plus the entry and exit Rogowski coils for current measurements, are immersed in a uniform axial magnetic field generated by a solenoid. The intensity of

the field  $B_0$  can be varied up to 10.5 kG.

The electrons are propagated in a stainless-steel drift tube with an inner diameter of 39 mm. The entire system is designed to operate in the fundamental  $TE_{11}$  mode of the cylindrical waveguide for which the cutoff frequency is 4.6 GHz. The beam current emerging from the emittance selector is illustrated in Fig. 3 as a function of the axial guide field  $B_0$ . At the resonance, when  $\lambda_0 \approx \lambda_w$ , the electrons have a large transverse excursion, strike the drift tube wall and are lost. From the experimental data we evaluate this resonance to be at its maximum at 4.7 kG. We observe in Fig. 3 that at a high  $B_0$  we have a good diode performance whereas the emission is perturbed when  $B_0$  is less than 3.5 kG. Consequently we ran our experiment in the group II regime. We note also the good agreement between the simulation and the experimental points with  $B_w = 0.5$  kG.

A high-power magnetron operating at 35.1 GHz is used as the input power source for the amplifier regime. The initial  $TE_{10}$  mode propagates through a standard  $Ka$ -band regular waveguide, and is then converted to a circular waveguide. This section of circular waveguide supports only the fundamental  $TE_{11}$  mode for the operating frequency. Its radius is then adiabatically uptapered to the radius of the drift tube. A tungsten wire grid launches the wave, without perturbing the electron orbits in the interaction region. The wave is linearly polarized, so that only half of the incident power, with the correct rotation of the electric field vector, participates in the FEL interaction. An attenuator allows us to reduce the usable power from a maximum of 20 kW to zero.

Just after the passage through the wiggler, a second tungsten wire grid deflects the rf power out of the drift tube, permitting the use of a Čerenkov diagnostic of the beam after its interaction with the electromagnetic wave. We also use this diagnostic to align the guiding coil with

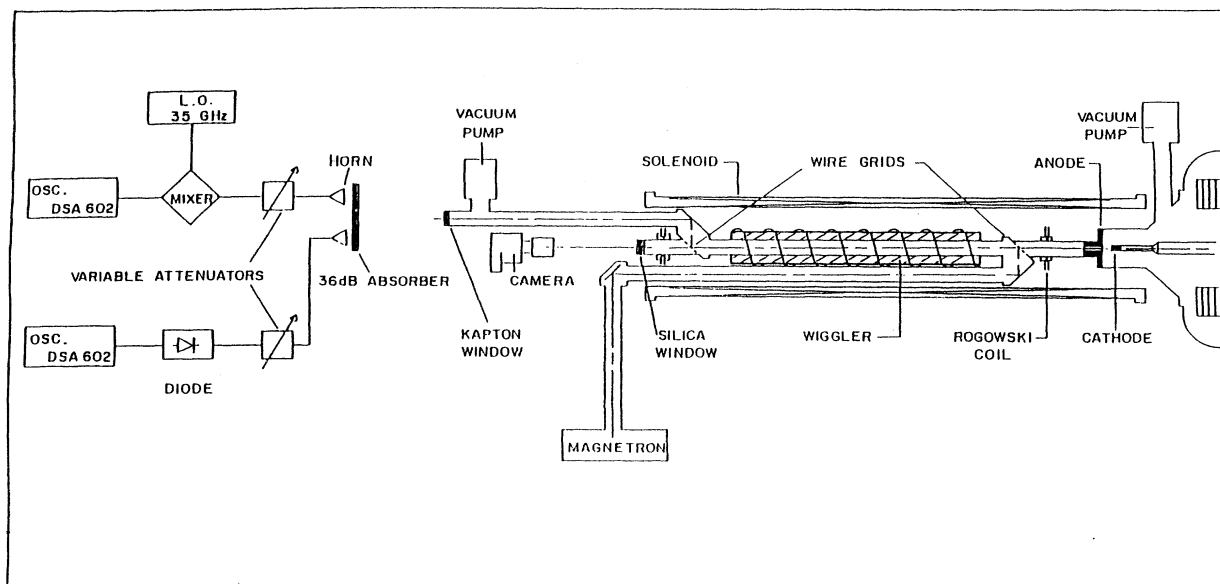


FIG. 1. Free-electron-laser experimental configuration.

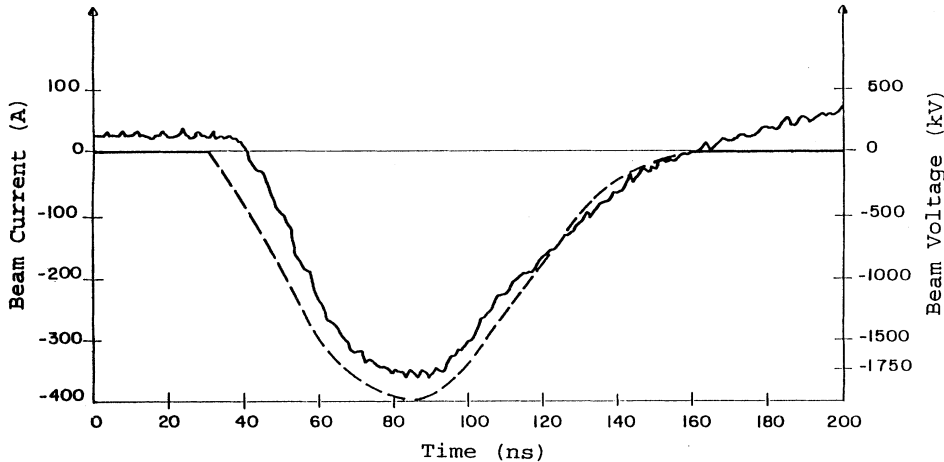


FIG. 2. Typical beam current (dashed line) and beam voltage (solid line) as a function of time.

the beam when the wiggler is turned off. The output power from the FEL is transmitted through a Kapton window which maintains the vacuum. After attenuation caused by spreading in the air and loss in a 36 dB absorber, a small fraction of the radiation is collected by a rectangular horn ( $Ka$  band). Then a variable attenuator (0–40 dB) reduces the power to the desired level for the diode detector whose response on the oscilloscope (Tektronix DSA-602) determines the power level. The entire system is calibrated using the known input power of the magnetron. Typical oscilloscope traces of the rf output signals are shown in Fig. 4 for two shots with the same parameters, but on different days. This shows that our experiment runs with a very good reproducibility.

A second channel with an identical horn and attenuator is used to measure the frequency. Less than 2 mW of the 35.1 GHz FEL radiation is mixed with radiation from a variable frequency 34–36 GHz local oscillator (LO). It is a Gunn-type diode which generates 10 mW at 35.9 GHz. The response of the mixer gives rise to the beat

wave of the two signals, and by varying the LO frequency we could explore the spectrum. This beat wave is then recorded by a 1 GHz passband oscilloscope and by a Fourier transformation we obtain the frequency spectrum. Results are shown in Fig. 5 for the parameter pair  $B_0 = 8$  kG and  $B_w = 0.95$  kG. The magnetron curve (a) exhibits a peak at 800 MHz corresponding to a 35.1 GHz frequency. We observe that the FEL signal in the amplifier regime (c) peaks exactly at 35.1 GHz just like that of the input magnetron. On the other hand, in the superradiant regime (b), although this main operating frequency is present it is mixed with other frequencies over a rather broadband. The full width at half maximum is less than 10 MHz for the magnetron corresponding to the 500 ns pulse length, and is approximately 100 MHz for the FEL radiation in consequence of the short pulse ( $\approx 10$  ns) emitted.

To find the optimum operating conditions, measurements of the output power with various choices of the magnetic fields have been carried out for both the super-

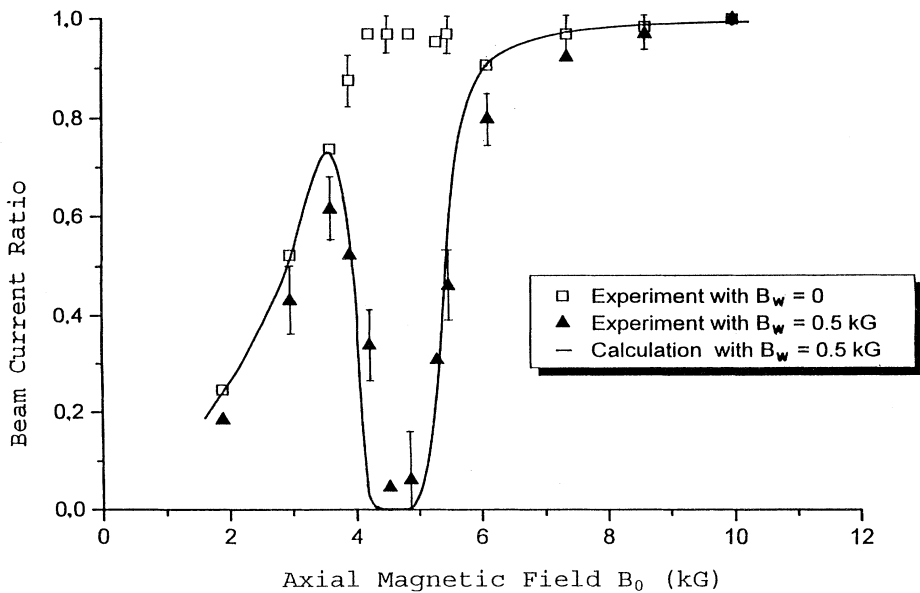


FIG. 3. FEL transmitted electron beam current as a function of the axial guide magnetic field  $B_0$  with a constant wiggler field  $B_w = 500$  G.

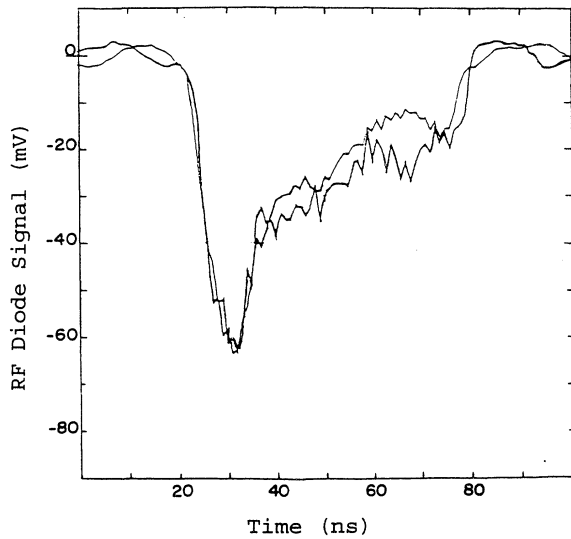


FIG. 4. FEL reproducibility; rf diode signal for  $B_0 = 10$  kG and  $B_w = 1.05$  kG.

radiant and the amplifier operation. The FEL output power as a function of  $B_w$  at constant  $B_0$  is illustrated in Fig. 6. Obviously the maximum output power is reached at the same  $B_w$  value for both operating regimes and the amplification factor is highest at this maximum. Nevertheless, the amplifier regime seems to show more sensitivity to  $B_w$  than the superradiant operation. One of the shots in the amplifier operation, which corresponds to the optimal choice of parameters  $B_0 = 8$  kG and  $B_w = 0.95$  kG, is represented in Fig. 7. Since 50 mV diode response corresponds to 5 mW and the variable attenuator is set for 100 dB in the total line attenuation (from the wiggler exit to the rf detector), this rf signal describes an output power level of 50 MW corresponding to an efficiency of 7% (the total electron beam power is 700 MW).

The study of the electromagnetic wave saturation was carried out by the measurement of the output power as a function of the interaction length in the wiggler. This length was varied by deflecting the electron beam into the drift tube wall. For this purpose, we use a movable coil which generates a transverse magnetic field greater than 1 kG. Figure 8 shows a measured gain curve, along with the simulation results for the optimum operating param-

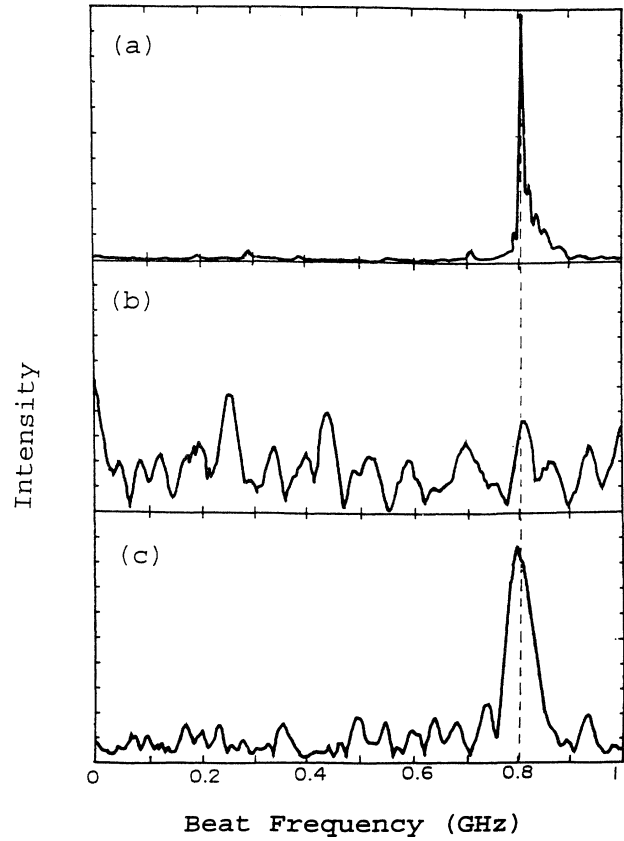


FIG. 5. Output power frequency spectrum: (a) magnetron alone, (b) superradiant regime, (c) amplifier regime.

eters defined previously. Comparison is made with the superradiant operation mode. When the geometrical emittance  $\epsilon$  is assumed to be  $500\pi$  mm mrad, the output power is observed to saturate at a length of 1.4 m, in good agreement with the simulation.

Saturation studies in the amplifier regime as a function of the input power have also been carried out. The FEL output power is given in Fig. 9 as a function of the magnetron input power. We see that less than 3 kW is enough to reach the experimental saturation, which corresponds to an amplification of 43 dB. The simulation using the single frequency code SOLITUDE correctly de-

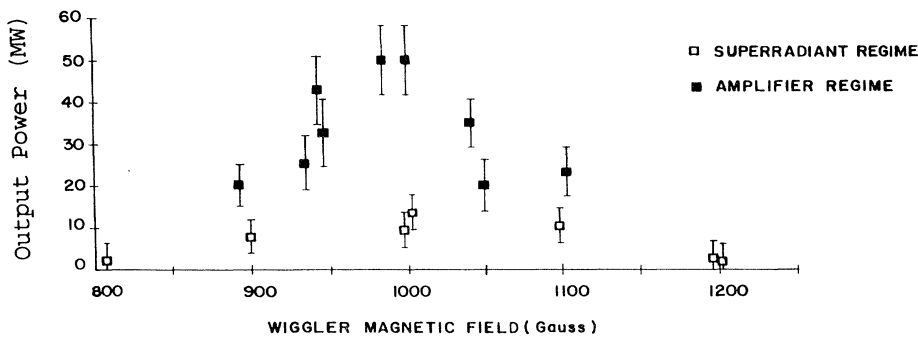


FIG. 6. FEL output power as a function of  $B_w$  for  $B_0 = 8$  kG.

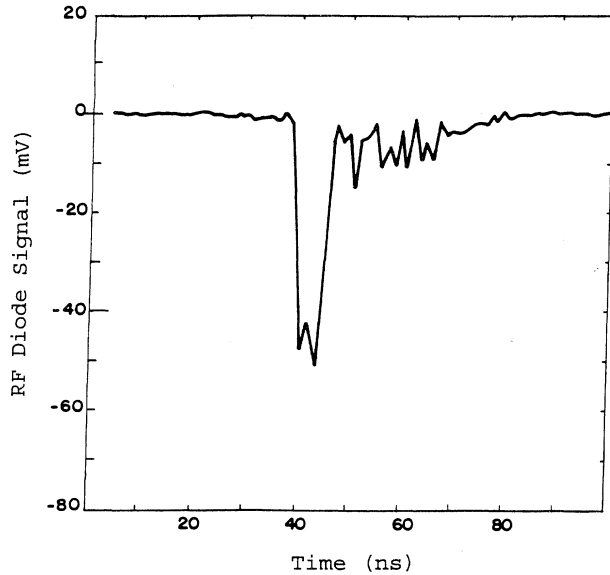


FIG. 7. rf diode signal for  $B_0 = 8$  kG and  $B_w = 0.95$  kG.

scribes the data corresponding to a real amplification (when the output power exceeds 15 MW), whereas at low input power the experiment runs as in the superradiant regime, yielding a broad spectrum in frequency. In the latter circumstance, the single frequency code underestimates the output power.

In order to find empirically the best operating conditions, the output power was measured over a two-dimensional domain of  $(B_0, B_w)$ . Some of the results are illustrated in Fig. 10, where the output power is shown as a function of  $B_0$  for the optimal value of  $B_w$  (shown in parentheses for each point). For comparison, the results of a simulation using the code SOLITUDE and assuming an ideal beam ( $\epsilon = 0$ ) are also given. The experimental results are seen to lie well below the simulation, essentially because of the relatively large emittance of our beam.

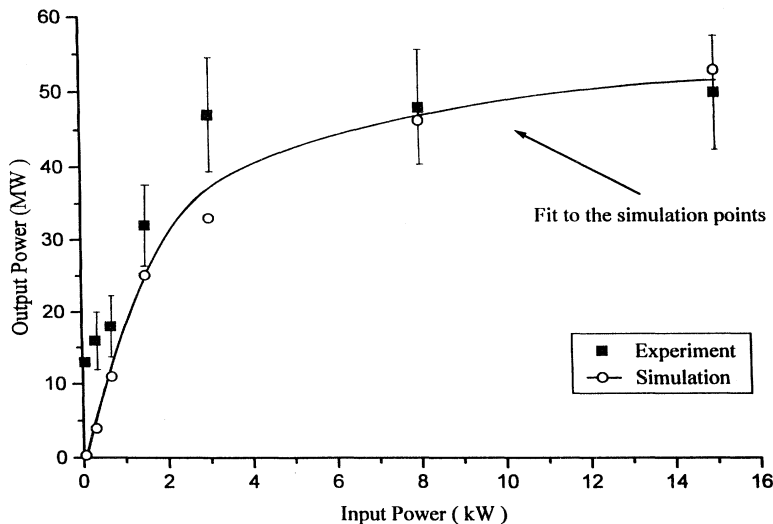


FIG. 9. FEL output power as a function of the magnetron input power.

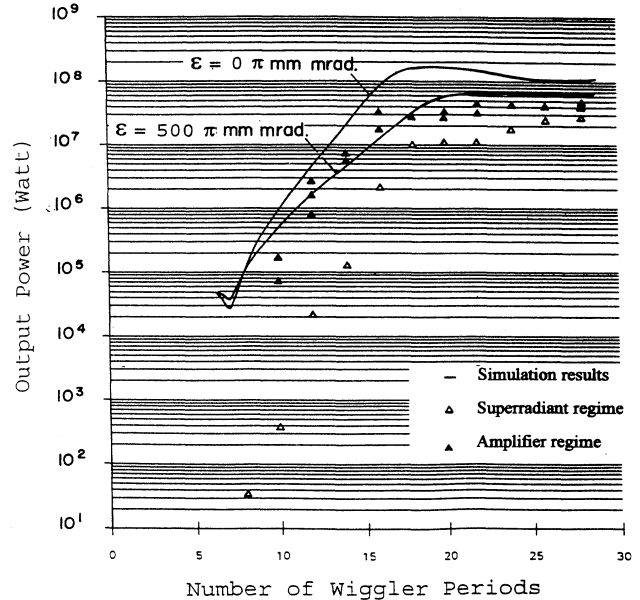


FIG. 8. Saturation studies for  $B_0 = 8$  kG and  $B_w = 0.95$  kG.

We suspect that another factor is the presence of other modes in the oversized guiding tube, although we cannot confirm this quantitatively.

### III. DISCUSSION

Before discussing our results, we wish to comment on some differences between this experiment and that carried out at the Naval Research Laboratory (NRL) and reported in Ref. [15]. The pulse generator available for our experiment was capable of producing beam energies as high as 5 MeV, and was therefore physically large. To a great extent, this fact required that the other components of the FEL be correspondingly oversized, as compared to the NRL experiment. The necessity of immersing the cathode of the large diode dictated the use of a large

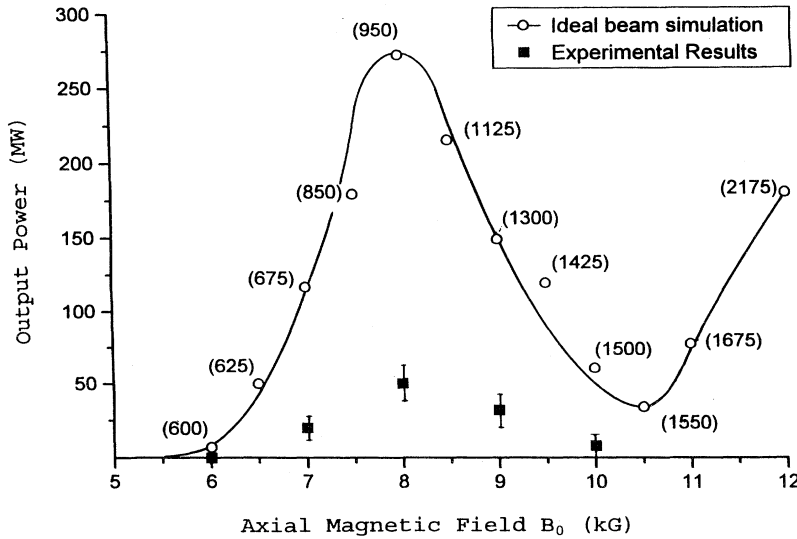


FIG. 10. FEL output power as a function of  $B_0$ , for the optimal value of  $B_w$  given in parenthesis.

aperture (200 mm diameter) solenoid, while the transverse size of the beam led to the choice of a 39 mm diameter cylindrical wave guide. The cutoff frequency for such a waveguide in the  $TE_{11}$  mode is 4.6 GHz, which is much less than the 35.1 GHz operating frequency of the magnetron we used. On the other hand, the use of the oversized components meant that the production of the axial and wiggler magnetic fields over large volumes required very high magnet currents, and the interesting large  $B_0$  region of operation could not be investigated. The available power supply limited the axial field to 10.5 kG, while our beam energy of 1.75 MeV meant that 35.1 GHz could be obtained with a step size of 80 mm for the wiggler. Typically the 35 GHz NRL experiment has a beam voltage of 0.9 MV, a 10.8 mm diameter waveguide and 30 mm wiggler wave length. Although these differences may appear to be minor, they in fact allowed our experiment to attain comfortably values of the coupling parameter  $\Phi$  which would have been hard to reach in the earlier experiments. Theoretical work by Freund and collaborators had previously indicated the desirability of investigating the regime of large and negative  $\Phi$ , and this was a major goal for us. Although it is theoretically possible to obtain arbitrarily large negative values of  $\Phi$  in any experiment by running sufficiently close to the limit of stability for group II, in practice a limit is set by the parasitic transverse oscillations about the ideal helical trajectory. These become large as one approaches the limits of stability, and under these conditions the electrons tend to hit the walls of the waveguide. In our experiment, the large diameter of the guide allows us to attain more negative values than previous ones. For example, the ideal helical orbit has a radius of about 5 mm, leaving room for transverse oscillations of as much as 14 mm. For the NRL experiment the comparable figures would be 2 and 3 mm, respectively. As an illustration of this we show in Fig. 11 a scatter plot of  $\Phi$  vs  $B_0$  for the pairs  $(B_0, B_w)$  studied in the present experiment (squares), together with our calculated  $\Phi$  for a typical range of  $(B_0, B_w)$  values which correspond to the experi-

ment of Gold *et al.* (solid curve, labeled NRL). Here the beam energies were fixed at the nominal values of 1.75 and 0.9 MeV, respectively. The arrows indicate those  $(B_0, \Phi)$  values where the maximum output power was obtained in the two experiments. It is clear that our experiment did reach larger negative values of  $\Phi$  than the NRL

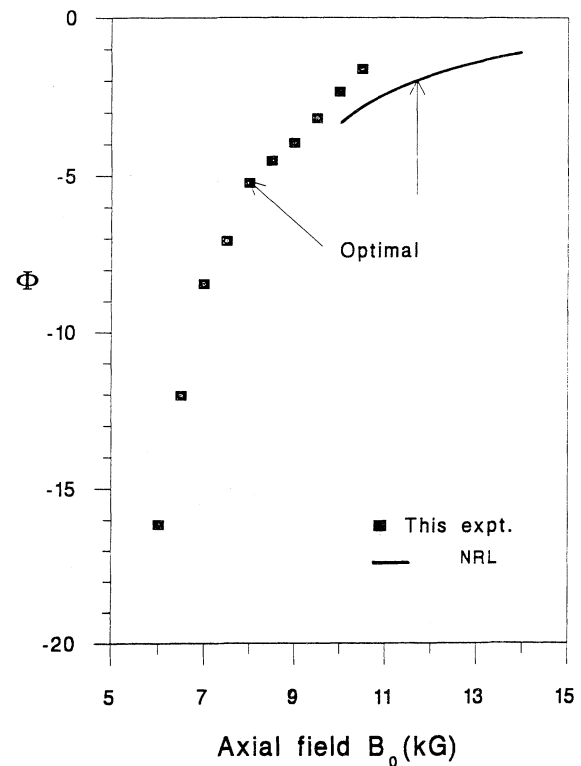


FIG. 11. The coupling parameter  $\Phi$  as a function of  $B_0$  for this experiment (squares), and for the range covered by the NRL experiment of Gold *et al.* (solid line). The arrows indicate where the maximum power was observed.

experiment. However, little amplification was observed in the extreme cases with  $\Phi < -8$ , and one may conclude that the high growth rate predicted for the large negative  $\Phi$  is offset by the practical disadvantage of working too near the limits of stability. Our experiment shows, in agreement with the NRL results, that the optimal choice of  $\Phi$  in the group II operation is not very large, and that extremely large negative values of  $\Phi$  are of no experimental interest.

Another difference between the experiments concerns the different diameters of the cylindrical waveguides used. The experiment of Gold *et al.* was designed to explore the region of "grazing incidence," where the two frequencies of the  $TE_{11}$  mode which can be in resonance with the propagating beam are approximately equal. In the present experiment, the cutoff frequency of 4.6 GHz is so far below the injected frequency of 35.1 GHz that the propagation in the guide is almost like in free space, and the lower frequency is approximately equal to the cutoff frequency. In addition, the large radius of our beam makes the plasma frequency much smaller, for a given beam current, than the NRL experiments. On the other hand, several other modes, notably  $TE_{01}$  and  $TE_{21}$ , may propagate at 35.1 GHz in our experiment, while this was not a problem for Gold *et al.* Unfortunately, our setup was not capable of measuring the angular distribution of output power with enough precision to demonstrate the presence of these other modes.

We have seen that the simulation of our experiment by the code SOLITUDE, provided an emittance of  $500\pi$  mm mrad is included, reproduces well the results. However, a simple explanation of the general features of the output power curve is provided by the model of Ref. [20]. At values of  $B_0 < 7$  kG, we are near the cyclotron resonance and the limits of stability for group II. Accordingly, the ideal helical electron orbits become unstable in the transverse direction and the rf power is close to zero. At  $B_0$  values of order 10 kG, the trajectories, although stable in the transverse direction, show very large oscillations (around 20%) in  $\beta_{\parallel}$ , as a function of  $z$ , due to the proximity of the double cyclotron resonance (which occurs when  $\beta_{\parallel} \approx \Omega_0 \lambda_w / 4\pi c$ ). This strongly oscillating longitudinal velocity is not suitable for interaction with the electromagnetic field, and again the output power is expected to be very small. Further increase in  $B_0$  beyond 11 kG should produce more rf power, but the magnet power supply was incapable of providing enough current for us to investigate this. Between these two regions where the electron trajectories are unsuitable for coherent interaction with the electromagnetic wave, we obtain a large amplification.

The frequency of the electromagnetic radiation obtained in the amplifier regime is expected to peak at the magnetron frequency of 35.1 GHz, as we have shown previously in Fig. 5. However, it was observed that this happened only for a small range of  $B_w$  at fixed  $B_0$ . For other values of  $B_w$ , the output frequency spectrum showed a number of peaks, separated by about 100 MHz.

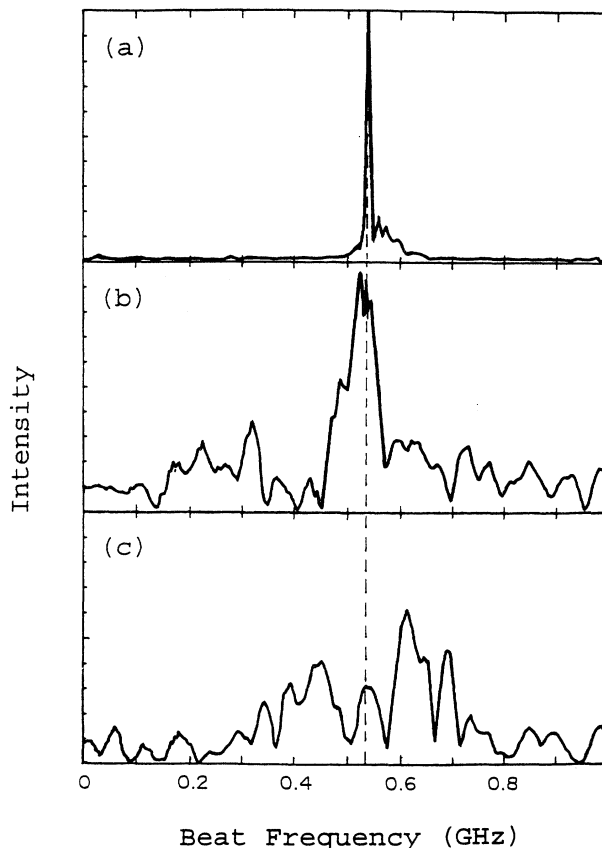


FIG. 12. Frequency spectrum (a) magnetron alone, (b) amplifier regime for  $B_w = 0.95$  kG and  $B_0 = 8$  kG, (c) amplifier regime for  $B_w = 1$  kG and  $B_0 = 8$  kG.

This is illustrated in Fig. 12, where the magnetron frequency spectrum in (a) (LO tuned at 35.63 GHz) and the output frequency spectrum for  $B_w = 0.95$  kG in (b) and  $B_w = 1$  kG in (c) are shown with  $B_0 = 8$  kG. The former displays a fairly compact spectrum centered on the magnetron frequency. In contrast, the latter shows a more complex spectrum, with adjacent peaks spaced by 100 MHz. We conjecture that these correspond, as in Ref. [21], to sidebands due to oscillations of the electrons in the ponderomotive potential.

In summary, we have carried out a successful high-power FEL experiment with a large negative coupling parameter  $\Phi$ . Operation in the amplifier mode at 35.1 GHz yielded 50 MW of output power with an efficiency of 7% for 43 dB of gain. The experimental results are in good agreement with predictions made using the 3D stationary simulation code SOLITUDE.

#### ACKNOWLEDGMENTS

The authors wish to thank E. Alozy, G. Marchese, and E. Pasini for their assistance in this work. They would also like to thank G. Bekefi for helpful discussions.

- [1] H. P. Freund and T. M. Antonsen, Jr., *Principles of Free-electron Lasers* (Chapman & Hall, London, 1992).
- [2] K. L. Felch *et al.*, IEEE J. Quantum Electron. **QE-17**, 1354 (1981).
- [3] R. K. Parker *et al.*, Phys. Rev. Lett. **48**, 238 (1982).
- [4] R. H. Jackson *et al.*, IEEE J. Quantum Electron. **QE-19**, 346 (1983).
- [5] J. Fajans, G. Bekefi, Y. Yin, and B. Lax, Phys. Rev. Lett. **53**, 246 (1984).
- [6] J. A. Pasour and S. H. Gold, IEEE J. Quantum Electron. **QE-21**, 845 (1985).
- [7] J. Masud *et al.*, Phys. Rev. Lett. **56**, 1567 (1986).
- [8] Y. Su *et al.*, Nucl. Instrum. Methods A **272**, 147 (1988).
- [9] M. E. Conde and G. Bekefi, Phys. Rev. Lett. **67**, 3082 (1991).
- [10] P. J. M. van der Slot and W. J. Witteman, Nucl. Instrum. Methods A **331**, 140 (1993).
- [11] K. Takayama *et al.*, Nucl. Instrum. Methods A **358**, 122 (1995).
- [12] L. Friedland and J. L. Hirshfield, Phys. Rev. Lett. **44**, 1456 (1980).
- [13] H. P. Freund *et al.*, Phys. Rev. A **26**, 2004 (1982).
- [14] H. P. Freund and A. K. Ganguly, Phys. Rev. A **28**, 3438 (1983).
- [15] S. H. Gold *et al.*, Phys. Rev. Lett. **52**, 1218 (1984).
- [16] S. H. Gold *et al.*, Phys. Fluids **27**, 746 (1984).
- [17] Ph. Gouard and J. Gardelle, Commissariat à l'Energie Atomique Report No. 5617, 1992 (unpublished).
- [18] J. Gardelle *et al.*, Phys. Rev. E **50**, 4973 (1994).
- [19] D. Prosnitz and E. T. Scharlemann, Lawrence Livermore National Laboratory ATA Note No. 229, 1984 (unpublished).
- [20] J. T. Donohue and J. L. Rullier, Phys. Rev. E **49**, 766 (1994).
- [21] F. G. Yee, J. Masud, T. C. Marshall, and S. P. Schlesinger, Nucl. Instrum. Methods A **259**, 104 (1987).